Life Sciences 291 (2022) 120263

Contents lists available at ScienceDirect

Life Sciences

journal homepage: www.elsevier.com/locate/lifescie

Small molecule STING inhibition improves myocardial infarction remodeling

Lavinia Rech [a], Mahmoud Abdellatif [a], Maria Pöttler [a], Verena Stangl [b], Nishani Mabotuwana [a,c,d], Sean Hardy [a,c,d], Peter P. Rainer [a,e,*]

[a] Division of Cardiology, Department of Internal Medicine, Medical University of Graz, Graz, Austria
[b] Diagnostic and Research Institute of Pathology, Medical University of Graz, Graz, Austria
[c] School of Medicine and Public Health, The University of Newcastle, Callaghan, Australia
[d] Hunter Medical Research Institute, New Lambton Heights, Australia
[e] BioTechMed Graz, Graz, Austria

ARTICLE INFO

Keywords:
cGAS
STING
Remodeling
Myocardial infarction
Inflammation
Fibrosis
Hypertrophy

ABSTRACT

Aims: Myocardial infarction (MI) is a major global cause of death. Massive cell death leads to inflammation, which is necessary for ensuing wound healing. Extensive inflammation, however, promotes infarct expansion and adverse remodeling. The DNA sensing receptor cyclic GMP-AMP synthase and its downstream signaling effector stimulator of interferon genes (cGAS-STING) is central in innate immune reactions in infections or autoimmunity. Cytosolic double-strand DNA activates the pathway and down-stream inflammatory responses. Recent papers demonstrated that this pathway is also active following MI and that its genetic targeting improves outcome. Thus, we investigated if pharmacologic pathway inhibition is protective after MI in order to test its translational potential.

Main methods: We investigated novel and selective small-molecule STING inhibitors that inhibit STING palmitoylation and multimerization and thereby downstream pathway activation in a preclinical murine MI model. We assessed structural and functional cardiac remodeling, infarct expansion and fibrosis, as well as cardiomyocyte hypertrophy and the expression of inflammatory genes.

Key findings: Pharmacologic STING inhibition did not reduce mortality due to myocardial rupture in non-reperfused MI. Infarct size at day one was comparable. However, three weeks of pharmacologic STING inhibition after reperfused MI decreased infarct expansion and scarring, increased left ventricular systolic function to levels approaching normal values, and reduced myocardial hypertrophy.

Significance: Selective small-molecule STING inhibition after myocardial infarction has the potential to improve wound healing responses and pathological remodeling and thereby attenuate the development of ischemic heart failure.

1. Introduction

Cardiovascular diseases (CVD) are the most common cause of death in the world [1]. Within these, the most prevalent are coronary artery disease and myocardial infarction (MI). Disruption of blood flow to the myocardium leads to acute and massive cell death. This results in the loss of cardiac contractility, collagenous scar formation, and ensuing progressive remodeling and heart failure.

Inflammation is a critical component of the wound healing response after myocardial necrosis. Inflammatory cells phagocytose cell and matrix debris and activate reparative pathways. However, this is a finely tuned process, and prolonged inflammation or activation of inflammatory pathways induce adverse remodeling responses and collateral damage. In general, pro-inflammatory and pro-reparative processes are balanced, and this involves both cellular and cytokine compartments of the innate and adaptive immune systems. Cytokines like Il-1β, Il-6, Il-18 or Tnfα are profoundly upregulated in proinflammatory phases, while in the pro-reparative phase, levels of e.g. Il-10 and Tgfβ increase [2].

* Corresponding author at: Division of Cardiology, Department of Medicine, Medical University of Graz, University Heart Center, Auenbruggerplatz 15, A-8036 Graz, Austria.
E-mail address: peter.rainer@medunigraz.at (P.P. Rainer).

https://doi.org/10.1016/j.lfs.2021.120263
Received 31 August 2021; Received in revised form 7 December 2021; Accepted 18 December 2021
Available online 28 December 2021

Damage-associated molecular patterns (DAMPs) are essential in the acute immune response after cell death [2]. Double-stranded DNA (dsDNA) is usually sequestered in the cell nucleus or mitochondria, however, if dsDNA is present outside of these organelles it can act as a DAMP. The DNA sensing receptor cyclic GMP-AMP synthase (cGAS) senses cytosolic dsDNA [3–5]. cGAS then synthetizes the second messenger cyclic guanosine monophosphate–adenosine monophosphate (cGAMP), which activates its downstream signaling effector, the endoplasmic reticulum resident protein stimulator of interferon genes (STING) [3,6]. Multimerization of STING receptors after activation results in the association with TANK-binding kinase 1 (TBK1) and its phosphorylation. This results in interferon regulatory factor 3 (IRF3) phosphorylation, which is a transcription factor for type I interferon (IFN). This pathway was first described in infectious and autoimmune diseases [3,7–13]. More recently, studies demonstrated that myocardial infarction and associated sterile inflammation also activate cGAS-STING [14]. cGAS and IRF3 knockout mice had improved survival after non-reperfused MI, and this was linked to the attenuated activity of pro-inflammatory macrophages [14,15]. Interestingly, mice genetically deficient in STING did not show improved post-MI survival [14]. In non-ischemic heart failure induced by murine pressure-overload, cGAS, STING, and their downstream chemokines Cxcl10 and Isg15 are upregulated early after banding [16]. Further, inhibiting cGAS reduces brain infarct volume after stroke [17], and inhibition of STING potently reduces expression of downstream chemokines [18,19].

STING inhibitors such as nitrofuran derivatives and indole ureas covalently bind to STING and inhibit cysteine palmitoylation thereby preventing STING multimer assembly, which is necessary for the phosphorylation of TBK1. The nitrofuran C-178 showed specific binding to mouse STING (mmSTING) and good inhibition of the pathway. The recently developed inhibitor H-151 (indole urea) antagonizes mmSTING and human STING (hsSTING) palmitoylation and reaches therapeutic drug concentrations in mice [19]. To our knowledge, none of these inhibitors was tested in MI remodeling before [20].

Thus, we here investigated if pharmacologic inhibition of STING using these novel and selective small-molecule STING palmitoylation inhibitors improves MI remodeling in order to probe their translational potential.

2. Methods

2.1. Ethics statement

Mouse handling and experiments were performed in agreement with the national and European ethical regulation (Directive 2010/63/EU), according to the guidelines of the Federation for Laboratory Animal Science Associations (FELASA) [21,22] and approved by the responsible government agencies Austria (Bundesministerium für Wissenschaft, Forschung und Wirtschaft, BMWFW, Austria: BMWF-66.010/0178-WF/V/3b/2017).

Animal experiments are reported following the ARRIVE guidelines (https://arriveguidelines.org/arrive-guidelines).

2.2. Animals

On average, 20 weeks-old male C57BL/6J mice purchased from Charles River Laboratories (Sulzfeld, Germany) were used. In total, we used 109 mice (79 mice for analyses). The remainder did not reach the end-point of the experiments or staining procedures failed. Animals were randomly assigned to experimental groups. Mice were housed in temperature-controlled rooms with a 12 h dark/light cycle with free access to water and food.

2.3. Myocardial infarction operation

Myocardial infarction was induced by left descending coronary artery (LAD) occlusion as described previously [23], using an Olympus SZX7 microscope (Japan). Briefly, mice were anaesthetized by isoflurane (Isofluran-Piramal, ATC-Code: N01AB06, Piramal Critical Care, UK) inhalation (5% for induction and 1.5–2% during the procedure) and orotracheally intubated (20 G) and mechanically ventilated (MiniVent Type 845, Hugo Sachs Elektronik, Germany), with additional i.p. injection of etomidate (10 mg/kg BW, Hypnomidate, ATC-Code: N01AX07, Janssen-Cilag Pharma GmbH, Austria) and buprenorphine (0.05 mg/kg BW Bupaq, ATC-Code: QN02AE01, Richter Pharma AG, Austria). Mice were placed on a temperature-controlled warming pad TC-1000 (CWE Inc., USA) to provide 37 °C body temperature and were connected to an electrocardiogram (ECG; Animal Bio Amp. FE136. ADInstruments, Australia) for heart rate control during the procedure.

The LAD was exposed by left transthoracic incision between the 4th–5th rib. The LAD was closed with a 7-0 monofilament Prolene (KHH5673SH Ethicon Inc., USA). The success of occlusion was assessed by myocardial blanching and ST elevation in ECG. Layer wise wound closure was performed with a 6-0 monofilament Prolene (EH8030H, Ethicon Inc., USA). Sham group was treated likewise but without LAD occlusion ($n = 16$ in total and analyses). Mice were either subjected to chronic total occlusion (non-reperfused) ($n = 40$ in total, $n = 27$ in analyses) or ischemia/reperfusion (I/R) ($n = 53$ in total, $n = 36$ in analysis) after 30 min of ischemia. Postoperative pain medication of buprenorphine (0.05 mg/kg BW Bupaq, ATC-Code: QN02AE01, Richter Pharma AG, Austria) was given in total for three days, three times a day subcutaneously.

2.4. Treatment

C57BL/6J mice were treated either with STING-Inhibitor or vehicle control daily with 200 μl intraperitoneal injection. The first injection was performed at the time of surgery. The inhibitor was dissolved in 10% Tween80 in isotonic saline solution with either 10% DMSO alone (control) or 10% Inhibitor C-178 or H-151 [19,24] (provided by Prof. A. Ablasser, EPFL Lausanne, Switzerland) solved in DMSO. Inhibitor C-178 was used for survival analysis. As it became available, we used the comparable inhibitor H-151 because of better solubility.

The abbreviations for the groups that we used were the following: myocardial infarction with treatment: MI-Inhib.; myocardial infarction with vehicle control: MI-CTL; Sham operated mice with treatment: Sham-Inhib.; Sham operated mice with vehicle control: Sham-CTL.

2.5. Echocardiography

Serial echocardiography was performed as previously described [25]. Briefly, mice were lightly anaesthetized with 0.5–1% Isoflurane and placed in the supine position on a temperature-controlled heating platform (VisualSonics mouse table, Fujifilm VisualSonic Inc., Canada) to maintain their body temperature at 37 °C. Images were acquired, using the high-resolution micro-imaging system Vevo 770 Imaging (VisualSonics Inc., Canada) equipped with a 45-Mhz linear array transducer (RMV 707B, VisualSonics Inc., Canada) on a Vevo 770 Imaging (VisualSonics Inc., Canada) to calculate endocardial systolic fractional area change (FAC) in parasternal long-axis views. Times of examination were baseline (before operation), one day postoperative and 21 days postoperative. For analysis, eleven mice in each group of MI-Inhib. and MI-CTL were used and five mice per group of Sham-Inhib. and Sham-CTL each.

2.6. Infarct volume

For evaluation of the primary infarct size, 2,3,5-Triphenyl-2H-tetrazolium chloride (TTC) and Evans blue were used. At day one after I/R surgery mouse hearts were explanted under deep anesthesia and pre-heparinization with 200 IE heparin. The aorta was cannulated and flushed with cold phosphate-buffered saline on ice to wash out

remaining blood. Afterwards, the LAD was re-closed ex vivo, and the heart was perfused with 1% Evans blue to determine the area at risk (perfused area). Then, the heart was sliced into 1 mm sections using the Zivic Matrix Heart Slicer (HSMS001-1, Zivic Instruments, USA) and incubated in 1.5% TTC solved in PBS for 15 min at 37 °C, followed by 4% formalin aldehyde after Lillie fixation at room temperature for maximal 90 min to determine the infarct size (necrotic area). Pictures were taken with an Olympus SZX12 microscope (Japan) and an Olympus DP21 camera (Japan). Images were analyzed for infarct size and area at risk (AAR) using the ImageJ software (National Institute of Health, USA). Four mice in each group (MI-Inhib. and MI-CTL) were used.

2.7. Quantitative real-time polymerase chain reaction (qPCR) analysis

RNA from heart tissue was isolated using QIAzol lysis reagent in MagNA Lyser Green Beats (03358941001, Roche Molecular Systems Inc., USA) and RNeasy kit (QIAGEN, Netherlands) according to the manual. RNA was quantified using a NanoDrop 2000 (Thermo Fisher Scientific, USA). 1 μg of RNA was used for the synthesis of cDNA utilizing the QuantiTect Reverse Transcription Kit (QIAGEN, Netherlands) according to the manufacturer's instructions. The assay was validated by generating standard curves to evaluate the efficiency of each primer set. The specificity of the PCR products was analyzed via melt curve and gel electrophoresis. qPCR runs were performed on the BIO RAD CFX384 (Bio-Rad, Japan) with SsoAdvanced Universal SYBR Green Supermix and primers (Table 1) was purchased by Ingenetix (Austria).

All reactions were performed in triplicates. Analysis of the gene expression levels was efficiency corrected and normalized to the reference genes 18s ribosomal RNA (18s) and hydroxymethylbilane synthase (Hmbs), calculated with the ΔΔCt method. Graphs were shown in the bars according to the $2^{-\Delta\Delta Ct}$ method and normalized to their control.

2.8. Histological analyses

For histological staining, formalin-fixed paraffin-embedded (FFPE) heart tissue (n = 3 each group) was used, cut with a rotation microtome (HM355S, ThermoFisher Scientific, USA) into 2 μm slices. Hematoxylin-eosin staining was performed with decreasing ethanol series (Xylol, 100% EtOH, 90%, 70%, 50%, aqua dest), hematoxylin (provided by the Core Facility Imaging, Centre for Medical Research Graz, Austria), eosin (provided by the Core Facility Imaging, Centre for Medical Research Graz, Austria), and increasing ethanol series (aqua dest, 50% EtOH, 70%, 90%, 100%) comparable as previously described [26].

Trichrome staining on 2 μm slices was performed using as following: Decreasing ethanol series, hematoxylin according to Gill, acidify with 0.5% acetic acid, staining with acid fuchsin, fixation with 1% phosphomolybdic acid, acidify with 0.5% acetic acid, staining with aniline blue, acidify with 0.5% acetic acid and finally increasing ethanol series.

Pictures were taken using the Panoramic P1000 Digital Slide Scanner (3D HISTEC Ltd., Hungary). Fibrosis quantification using the trichrome images were analyzed using ImageJ software (National Institute of Health, USA).

For WGA staining, slices from 2 μm thickness, cut with a rotation microtome (HM355S, ThermoFisher Scientific, USA) from FFPEs, were deparaffinized and rehydrated. Antigen retrieval using sodium citrate + 0.5% Tween 20 at a pH 6 were performed. Wheat germ agglutination (WGA, Alexa Fluor 555, W32464, Invitrogen, USA) staining was conducted with a 1:200 dilution for 1 h at room temperature. Slices were covered using GLC mounting medium (1408, Sakura Finetek, Japan) drying for 24 h at room temperature.

Images were taken using the Olympus BX51 fluorescence microscope (Olympus, Japan) with a CY3 filter (513–556 nm). These were analyzed using 20× magnified pictures and the ImageJ software (National Institute of Health, USA). Four orthogonal spots (each 5.5 × 10^5 μm^2) of every slice have been analyzed using 'analyze particles' with a size cutoff of 100–550 μm^2 and a circularity of 0.25–1.00.

Table 1
Primers used for qPCR.

Gene	Abbreviation	Forward	Reverse
Interleukin 6	Il6	TTG GTC CTT AGC CAC TCC TTC	TTG GTC CTT AGC CAC TCC TTC
Natriuretic peptide type A	Nppa	GCT TCC AGG CCA TAT TGG AG	GGG GGC ATG ACC TCA TCT T
Natriuretic peptide type B	Nppb	GAG GTC ACT CCT ATC CTC TGG	GCC ATT TCC TCC GAC TTT TCT C
Myosin, heavy polypeptide 6, cardiac muscle, alpha	Myh6	GCC CAG TAC CTC CGA AAG TC	GCC TTA ACA TAC TCC TCC TTG TC
Tumor necrosis factor alpha	Tnfα	GAG AGT GGT CAG GTT GCC TC	GCA CCT CAG GGA AGA ATC TGG
Transforming growth factor beta 1	Tgfβ1	CAG GAC CTG AGG ACT CCA GA	GGA ATA GGG GCG TCT GAG GA
Transforming growth factor beta 2	Tgfβ2	CGA GGA GTA CTA CGC CAA GG	GGA TGG CAT TTT CGG AGG GG
Myosin, heavy polypeptide 7, cardiac muscle, beta	Myh7	GTG CCC GAT GAC AAA GAA GAG TTT G	CTT GCC ATT CTC CGT CTC AGC
Interferon-induced protein with tetratricopeptide repeats 2	Ifit2	GAG TAC AAC GAG TAA GGA GTC ACT GG	CAT CCT TGT TAA ACA CCC TGT CCT C
Interferon-induced protein 44	Ifi44	CTG GAG GCA TTC CAT GGA GTC TTT G	GAG GAT CAG CAT GTC CTT CAC G
Interleukin 1 beta	Il1β	CTG CAG CTG GAG AGT GTG G	GGG GAA CTC TGC AGA CTC AA
Chemokine (C-X-C-motif) ligand 10	Cxcl10	CAA GTG CTG CCG TCA TTT TCT G	GAT ATG GAT GCA GTT GCA GCG G
ISG15 ubiquitin-like modifier	Isg15	CAG TGC TCC AGG ACG GTC TTA C	CTT TCG TTC CTC ACC AGG ATG C
Collagen type 1 alpha 1	Col1a1	CCT GTG TGT TCC CTA CTC AGC	GGA ATC CAT CGG TCA TGC TCT C
Collagen type 1 alpha 2	Col1a2	GGA GGG AAC GGT CCA CGA TTG	GAG TCC GCG TAT CCA CAA AGC
Collagen type 3 alpha 1	Col3a1	GAA GGC GAA TTC AAG GCT GAA GG	GGG TAG TCT CAT TGC CTT GCG T
Hydroxymethylbilane synthase (Ref gene)	Hmbs	GGG TGA TTC GAG TGG GCA C	CTC CCG TGG TGG ACA TAG CA
18s ribosomal RNA (small ribosomal subunit component) (Ref gene)	18s	GTA ACC CGT TGA ACC CCA TT	CCA TCC AAT CGG TAG TAG CG

2.9. Statistical analyses

All data are shown in mean ± standard error of the mean (SEM). Outliers were identified using the ROUT method with Q = 1%. Interactions of more than two groups were compared with two-way ANOVA or Kruskal-Wallis-Test as appropriate, both with a Bonferroni post hoc test for multiple comparisons, normality was tested by Shapiro-Wilk test. Comparing two groups with normal distribution two-tailed *t*-test was used in all others Mann-Withney-*U* Test. Statistical significance was taken if $p < 0.05$. All analyses were performed with GraphPad Prism 8 software (GraphPad Software Inc., USA).

3. Results

3.1. Pharmacologic STING inhibition does not improve early MI survival

First, we exposed mice to non-reperfused myocardial infarction. This leads to large infarcts and a substantial proportion of ensuing myocardial rupture and death. We administered STING inhibitor C-178 at the time of infarction and monitored mortality. Survival analysis over 24 days showed no impact of STING inhibition on early post-MI survival (MI-Inhib; $n = 10$) and controls (MI-CTL, n = 10) (Fig. 1) with the high proportion of death due to myocardial rupture typical for large non-reperfused MIs [23]. Analysis of cytokines (Suppl. Fig. 1) and remodeling markers did not show significant differences at day 4 after MI. Thus, STING inhibition did not rescue early mortality in large non-reperfused MIs.

3.2. STING-inhibition improves cardiac remodeling in reperfused myocardial infarction

To mimic the clinical scenario and assess cardiac remodeling responses in a less severe ischemia model, we subsequently employed the myocardial ischemia/reperfusion (I/R) model where the LAD is temporally occluded. This corresponds to clinics, where we seek to revascularize occluded coronaries as soon as possible. Mice were subjected to 30 min of myocardial ischemia with or without concomitant STING inhibition. The initial area at risk and infarct size were comparable (Fig. 2A+B) as was impairment of left ventricular function (Fig. 2C).

However, after three weeks, echocardiography demonstrated significant improvement in left ventricular systolic function in mice treated with inhibitor H-151 (Fig. 2C+D, Suppl. Table 1, Suppl. Fig. 2, $p = 0.045$). Systolic function in treated mice was comparable to values seen in sham-operated animals. Corresponding to improved functional outcome, histologic examination demonstrated less cardiomyocyte hypertrophy (Fig. 2E+G; $p = 0.002$) and reduced collagen deposition and scarring in the infarct area (Fig. 2F+G, Suppl. Fig. 3; $p = 0.013$).

3.3. Expression patterns of inflammatory genes

The universal pro-inflammatory cytokines Il1β and Il6 show a robust induction persisting three weeks after I/R compared to shams (Fig. 3A) and this was not changed by STING inhibition. However, when assaying the more specific IFN-induced genes Ifi44 and Cxcl10 we saw persistent downregulation in the inhibitor group ($p = 0.025$ and $p = 0.021$, respectively) (Fig. 3B).

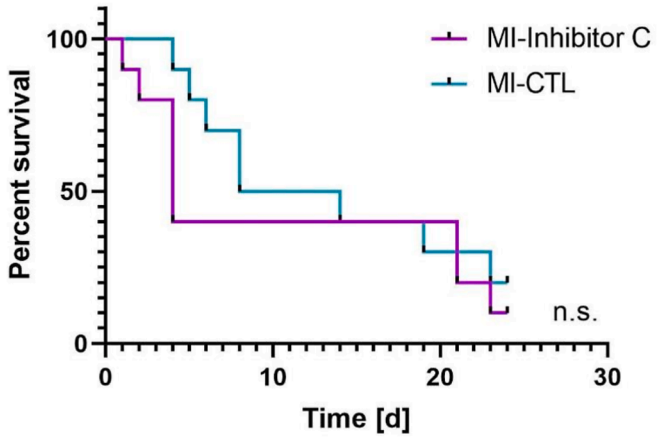

Fig. 1. STING inhibition does not rescue mortality in non-reperfused MIs. $n = 10$ per group. The experiment ended at day 24 after non-reperfused MI. Inhibitor C=C-178.

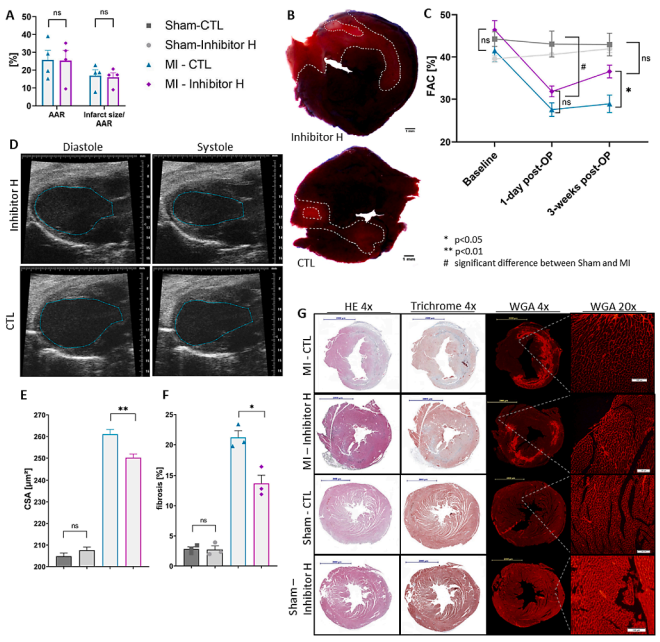

Fig. 2. Phenotypic characterization of H-151's effect on early remodeling after reperfused MI. (A) Quantification and (B) representative images of infarct size and area at risk (infarct white, area at risk red) at day 1. (C) Left ventricular function assessed by endocardial systolic fractional area change (FAC). MI induces left ventricular dysfunction to a similar extent in both groups but H-151 treatment for 3 weeks improves FAC back towards normal values (MI groups $n = 11$ each; Sham groups $n = 5$ each, $p = 0.045$ between MI-Inh. and MI-CTL) (D) Representative echocardiograms in parasternal long axis view (E) Myocyte cross sectional area ($n = 3$ hearts per group, >1100 cells per heart, $^{**}p = 0.002$) (F) Collagen area fraction (n = 3 hearts per group, $^{*}p = 0.013$). (G) Representative images for HE, Masson Trichrome, and WGA stainings. Scale bar 2 mm (2000 µm) in 4×; scale bar 100 µm in 20×. Inhibitor H=H-151. (For interpretation of the references to colour in this figure legend, the reader is referred to the web version of this article.)

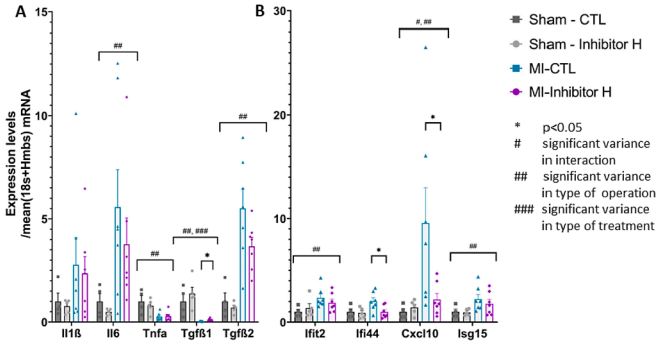

Fig. 3. Gene expression in the infarct zone at 3 weeks after reperfused MI. (A) Tgfβ1 expression was reduced in the infarct zone but less so in inhibitor-treated mice ($p = 0.026$). (B) STING inhibition decreased expression of IFN-induced genes Ifi44 ($^{*}p = 0.025$) and Cxcl10 ($^{*}p = 0.021$). Inhibitor H=H-151.

4. Discussion

cGAS-STING is a known innate immune regulatory pathway in infections, autoimmunity, and cancer. Recently, studies investigated the role of this pathway in cardiovascular disease. Genetic deletion of cGAS in mice ($cGAS^{-/-}$) improved systolic function following non-reperfused MI [14,15] and non-ischemic pressure-overload-induced heart failure [27]. Interestingly, in the study by King and coworkers, genetic loss of STING function ($STING^{gt/gt}$) did not improve post-MI systolic left ventricular function nor survival despite reduced expression of interferon

induced genes such as Cxcl10 or Ifi44. In contrast, IRF-3 knockout within the same study ameliorated both post-MI function and survival [14]. In our hands, small molecule STING inhibition selectively reduced Cxcl10 and Ifi44 expression. In addition, pharmacologic STING inhibition substantially improved cardiac function three weeks after I/R and significantly reduced collagen deposition and scarring in the infarct zone. However, it did not alter short-term mortality. Aside from the mode of cGAS-STING inhibition (genetic vs. small molecule pharmacological) also the model (I/R vs. non-reperfused MI) and timing of experiments differed between studies. In addition, in order to assess survival following I/R, where infarct sizes are much smaller and early mortality is low, long term studies with larger sample sizes are needed. We expect that improved function and less scarring leads to improved survival, however, this remains to be tested. In the study by Cao and coworkers, cGAS$^{-/-}$ mice also had improved survival and function post-MI [15]. Interestingly, they observed increased deposition of soluble (not cross-linked) collagen in the infarct scar at one week and attribute the improved survival to facilitated scar formation and reduced risk of myocardial rupture [15]. Both studies related the protective effect to modulation of cardiac macrophage phenotypes by cGAS-STING (proreparative vs. inflammatory [15], interferon-inducible cell (IFNIC) cardiac macrophages [14]). This is consistent with a recent paper from Pham et al., which investigated cGAS-STING signaling in atherosclerosis. STING was up-regulated in macrophages in atherosclerotic lesions in mice and humans and genetic STING or pharmacologic inhibition with the nitrofuran derivative C-176 reduced atherogenesis in Apoe$^{-/-}$ mice. Myeloid cell specific re-expression of STING in STING$^{-/-}$ Apoe$^{-/-}$ double knockout mice promoted atherogenesis [28].

Another myeloid cell type that is critically involved in MI wound healing is neutrophils. Zhang et al. described that reducing N1 neutrophils in the infarct zone reduces infarct size and increases systolic function [29]. Furthermore, Liu et al. showed that mtDNA increases neutrophil extracellular trap (NET) formation via STING [30]. Aside from cardiac injury, Li et al. found that cGAS-STING inhibition with the oligodeoxynucleotide A151 reduced neutrophil infiltration and infarct size in ischemic stroke and improved neurological outcomes [17].

Hu et al. used a non-ischemic heart failure model, i.e. pressure-overload through transverse aortic constriction (TAC) [16]. They show cGAS-STING induction in that model despite the absence of massive cell death and concomitant massive release of DAMPs such as dsDNA. Silencing cGAS by using an AAV-9 vector improved survival and function, reduced hypertrophy and fibrosis, and reduced macrophage infiltration at one week after TAC.

Here, we confirm the protective effect of cGAS-STING pathway interference that was seen in genetic mouse models exposed to acute myocardial infarction or non-ischemic heart failure by using selective pharmacologic STING inhibition. Thus, there is clear translational potential for this approach in acute MI remodeling to prevent infarct expansion and ensuing ischemic cardiomyopathy and heart failure. Importantly, post-MI remodeling is a dynamic process where early massive cell death and inflammation is followed by scar formation, maturation and later chronic adaptation of the remote myocardium to the loss of contractile tissue. Thus, future studies need to address optimal timing of STING inhibition in order to maximize benefit. However, the fact that cGAS-STING inhibition was also effective in non-ischemic heart failure [16] is encouraging, as the early acute wound healing response present in MI healing is absent in this model. This suggests that this approach may be beneficial both early after MI (as seen with genetic models and our study) and in chronic heart failure remodeling. The translational potential is substantial as cGAS-STING modulation has received much attention recently and novel drug therapies based on this pathway are currently being developed [31].

5. Strengths and limitations

Our study was an exploratory study to test the hypothesis that pharmacologic selective STING inhibition is capable to improve acute MI remodeling as suggested by prior studies using genetic means. By using pharmacologic inhibition in an integrated in vivo model we add to prior studies and increase translational value. We did not study the underlying inflammatory and cell specific response in detail, however, the observed changes in IFN-induced genes suggest that the mechanisms are similar to the ones observed in prior work [14,15]. Furthermore, we did not investigate individual cell types involved in cardiac remodeling or metabolic parameters and blood pressure. In another study, STING inhibition did not alter blood pressure or metabolic parameters [28]. Additionally, as post-MI healing is a dynamic process comprising both acute wound healing and chronic remodeling responses we need future studies to address correct timing of treatment. Lastly, we used only male mice. Future studies in female mice need to determine if our findings can be generalized.

6. Conclusions

Pharmacologic STING inhibition reduces infarct expansion and scarring after myocardial infarction and improves left ventricular function and hypertrophy. The translational potential is substantial and needs to be probed in further studies.

CRediT authorship contribution statement

L.R., M.A., M.P., V.S., N.M., and S.H. performed experimental work, L.R., M.A., and P.P.R. analyzed and interpreted data. L.R. and P.P.R. designed the study, L.R. and P.P.R. wrote the manuscript. All authors have contributed, edited, and agreed to the published version of the manuscript.

Funding

This research was funded in whole, or in part, by ERA-CVD and the Austrian Science Fund (FWF) [AIR-MI project: I 4168-B to P.P.R.] and the Austrian Society of Cardiology [to P.P.R.]. Lavinia Rech was trained within the frame of the PhD Program Molecular Medicine of the Medical University of Graz. For the purpose of open access, the author has applied a CC BY public copyright license to any author accepted manuscript version arising from this submission.

Declaration of competing interest

The authors declare that the research was conducted in the absence of any commercial or financial relationships that could be construed as a potential conflict of interest.

Acknowledgments

We thank Eva Ulcar (Diagnostic and Research Institute of Pathology, Medical University of Graz, Graz, Austria) and Viktoria Trummer-Herbst (Department of Internal medicine, Division of Cardiology, Medical University of Graz, Graz, Austria) for expert technical assistance and Andrea Ablasser and Muhammet F. Gülen (Global Health Institute, Ecole Polytechnique Fédérale de Lausanne, Lausanne, Switzerland) for providing reagents. The graphical abstract was created with BioRender.com.

Appendix A. Supplementary data

Supplementary data to this article can be found online at https://doi.org/10.1016/j.lfs.2021.120263.

References

[1] N. Townsend, L. Wilson, P. Bhatnagar, K. Wickramasinghe, M. Rayner, M. Nichols, Cardiovascular disease in Europe: epidemiological update 2016, Eur. Heart J. 37 (42) (2016) 3232–3245, https://doi.org/10.1093/eurheartj/ehw334.

[2] N.G. Frangogiannis, Cell biological mechanisms in regulation of the post-infarction inflammatory response, Curr. Opin. Physiol. 1 (2018), https://doi.org/10.1016/j.cophys.2017.09.001.

[3] X. Cai, Y.H. Chiu, Z.J. Chen, The cGAS-cGAMP-STING Pathway of Cytosolic DNA Sensing and Signaling vol 54, 2014, 10974164.

[4] L. Sun, J. Wu, F. Du, X. Chen, Z.J. Chen, Cyclic GMP-AMP synthase is a cytosolic DNA sensor that activates the type I interferon pathway, Science 339 (6121) (2013) 786–791, https://doi.org/10.1126/science.1232458.

[5] J. Wu, L. Sun, X. Chen, F. Du, H. Shi, C. Chen, et al., Cyclic GMP-AMP is an endogenous second messenger in innate immune signaling by cytosolic DNA, Science 339 (6121) (2013) 826–830, https://doi.org/10.1126/science.1229963.

[6] A. Ablasser, M. Goldeck, T. Cavlar, T. Deimling, G. Witte, I. Röhl, et al., CGAS produces a 2′-5′-linked cyclic dinucleotide second messenger that activates STING, Nature 498 (7454) (2013) 380–384, https://doi.org/10.1038/nature12306.

[7] J.W. Schoggins, D.A. MacDuff, N. Imanaka, M.D. Gainey, B. Shrestha, J.L. Eitson, et al., Pan-viral specificity of IFN-induced genes reveals new roles for cGAS in innate immunity, Nature 505 (7485) (2014) 691–695, https://doi.org/10.1038/nature12862.

[8] X.-D. Li, J. Wu, D. Gao, H. Wang, L. Sun, Z.J. Chen, in: Pivotal Roles of cGAS-cGAMP Signaling in Antiviral Defense and Immune Adjuvant Effects 341(6152), 2013, pp. 1390–1394, 10959203.

[9] D. Wan, W. Jiang, J. Hao, Research advances in how the cGAS-STING pathway controls the cellular inflammatory response, Front. Immunol. 11 (2020) 615, https://doi.org/10.3389/fimmu.2020.00615.

[10] H. Liu, P. Moura-Alves, G. Pei, H.-J. Mollenkopf, R. Hurwitz, X. Wu, cGAS facilitates sensing of extracellular cyclic dinucleotides to activate innate immunity, EMBO Rep. 20 (4) (2019), https://doi.org/10.15252/embr.201846293.

[11] D. Gao, T. Li, X.-D. Li, X. Chen, Q.-Z. Li, M. Wight-Carter, et al., Activation of cyclic GMP-AMP synthase by self-DNA causes autoimmune diseases, Proc. Natl. Acad. Sci. U. S. A. 112 (42) (2015) E5699–E5705, https://doi.org/10.1073/pnas.1516465112.

[12] T. Li, Z.J. Chen, The cGAS-cGAMP-STING pathway connects DNA damage to inflammation, senescence, and cancer, J. Exp. Med. 215 (5) (2018) 1287–1299, https://doi.org/10.1084/jem.20180139.

[13] J. Ahn, D. Gutman, S. Saijo, G.N. Barber, STING manifests self DNA-dependent inflammatory disease, Proc. Natl. Acad. Sci. 109 (47) (2012) 19386–19391, https://doi.org/10.1073/pnas.1215006109.

[14] K.R. King, A.D. Aguirre, Y.X. Ye, Y. Sun, J.D. Roh, R.P. Ng, et al., IRF3 and type I interferons fuel a fatal response to myocardial infarction, Nat. Med. 23 (12) (2017) 1481–1487, https://doi.org/10.1038/nm.4428.

[15] D.J. Cao, G.G. Schiattarella, E. Villalobos, N. Jiang, H.I. May, T. Li, et al., Cytosolic DNA sensing promotes macrophage transformation and governs myocardial ischemic injury, Circulation 137 (24) (2018) 2613–2634, https://doi.org/10.1161/CIRCULATIONAHA.117.031046.

[16] D. Hu, Y.-X. Cui, M.-Y. Wu, L. Li, L.-N. Su, Z. Lian, et al., Cytosolic DNA sensor cGAS plays an essential pathogenetic role in pressure overload-induced heart failure, Am. J. Physiol. Heart Circ. Physiol. 318 (6) (2020) H1525–H1537, https://doi.org/10.1152/ajpheart.00097.2020.

[17] Q. Li, Y. Cao, C. Dang, B. Han, R. Han, H. Ma, et al., Inhibition of double-strand DNA-sensing cGAS ameliorates brain injury after ischemic stroke, EMBO Mol. Med. 12 (4) (2020), e11002, https://doi.org/10.15252/emmm.201911002.

[18] S. Li, Z. Hong, Z. Wang, F. Li, J. Mei, L. Huang, et al., The cyclopeptide astin C specifically inhibits the innate immune CDN sensor STING, Cell Rep. 25 (12) (2018) 3405–3421, https://doi.org/10.1016/j.celrep.2018.11.097, e7.

[19] S.M. Haag, M.F. Gulen, L. Reymond, A. Gibelin, L. Abrami, A. Decout, et al., Targeting STING with covalent small-molecule inhibitors, Nature (2018), https://doi.org/10.1038/s41586-018-0287-8.

[20] L. Rech, P.P. Rainer, The innate immune cGAS-STING-pathway in cardiovascular diseases – a mini review, Front. Cardiovasc. Med. 8 (2021), https://doi.org/10.3389/fcvm.2021.715903.

[21] J. Guillen, FELASA guidelines and recommendations, J. Am. Assoc. Lab. Anim. Sci. 51 (2012).

[22] H.-M. Voipio, P. Baneux, I.A. Gomez de Segura, J. Hau, S. Wolfensohn, Guidelines for the veterinary care of laboratory animals: report of the FELASA/ECLAM/ESLAV joint working group on veterinary care, Lab. Anim. 42 (1) (2008) 1–11, https://doi.org/10.1258/la.2007.007027.

[23] P.P. Rainer, S. Hao, D. Vanhoutte, D.I. Lee, N. Koitabashi, J.D. Molkentin, et al., Cardiomyocyte-specific transforming growth factor \beta suppression blocks neutrophil infiltration, augments multiple cytoprotective cascades, and reduces early mortality after myocardial infarction, Circ. Res. 114 (8) (2014) 1246–1257, https://doi.org/10.1161/CIRCRESAHA.114.302653.

[24] A. Decout, J.D. Katz, S. Venkatraman, A. Ablasser, The cGAS-STING Pathway as a Therapeutic Target in Inflammatory Diseases, 2021, https://doi.org/10.1038/s41577-021-00524-z, 14741741.

[25] T. Eisenberg, M. Abdellatif, S. Schroeder, U. Primessnig, S. Stekovic, T. Pendl, et al., Cardioprotection and lifespan extension by the natural polyamine spermidine, Nat. Med. 22 (12) (2016) 1428–1438, https://doi.org/10.1038/nm.4222.

[26] R.D. Cardiff, C.H. Miller, R.J. Munn, Manual hematoxylin and eosin staining of mouse tissue sections, Cold Spring Harb Protoc 2014 (6) (2014) 655–658, https://doi.org/10.1101/pdb.prot073411.

[27] Y. Zhang, W. Chen, Y. Wang, STING is an essential regulator of heart inflammation and fibrosis in mice with pathological cardiac hypertrophy via endoplasmic reticulum (ER) stress, Biomed. Pharmacother. 125 (2020), 110022, https://doi.org/10.1016/j.biopha.2020.110022.

[28] P.T. Pham, D. Fukuda, S. Nishimoto, J.-R. Kim-Kaneyama, X.-F. Lei, Y. Takahashi, et al., STING, a cytosolic DNA sensor, plays a critical role in atherogenesis: a link between innate immunity and chronic inflammation caused by lifestyle-related diseases, Eur. Heart J. (2021), https://doi.org/10.1093/eurheartj/ehab249.

[29] Y. Zhang, W. Wen, H. Liu, The role of immune cells in cardiac remodeling after myocardial infarction, J. Cardiovasc. Pharmacol. 76 (4) (2020) 407–413, https://doi.org/10.1097/FJC.0000000000000876.

[30] L. Liu, Y. Mao, B. Xu, X. Zhang, C. Fang, Y. Ma, et al., Induction of neutrophil extracellular traps during tissue injury: involvement of STING and toll-like receptor 9 pathways, Cell Prolif. 52 (3) (2019), e12579, https://doi.org/10.1111/cpr.12579.

[31] C. Sheridan, Drug developers switch gears to inhibit STING, Nat. Biotechnol. 37 (3) (2019) 199–201, https://doi.org/10.1038/s41587-019-0060-z.